

Enhancement of an Electrified Tilt-Wing Propulsion System using Turbine Electrified Energy Management

Jonathan L. Kratz¹ and Dennis E. Culley²
NASA Glenn Research Center, Cleveland, Ohio, 44135, U.S.A.

Hybrid gas-electric aircraft propulsion architectures provide flexibility in the way that power and energy is managed when compared to their traditional pure-gas counterparts. In this paper, investigations are conducted for the impact this added flexibility has on the operability of turbomachinery. Specifically, the Turbine Electrified Energy Management (TEEM) concept is applied. It takes a controls approach to improving operability of the turbomachinery by utilizing electric hardware. In this paper, TEEM is applied to a propulsion system for a 15 passenger vertical lift concept vehicle. This is the first application of TEEM to a turbine engine that generates power. The study establishes TEEM as being applicable to this smaller thrust/power class of air transportation vehicle and explores how power can be otherwise managed in the propulsion system to benefit the aircraft. The simulation study demonstrates significant improvements in transient operability that expands the engine design space to enable a more efficient and lighter-weight engine design. Simulation results also demonstrate tighter regulation of the power turbine and rotor speeds, a slight decrease in bulk fuel burn, and an increase in the maximum thrust of ~7%. This is achieved through the power management control strategy and modestly sized electric machines with re-usable energy storage.

I. Nomenclature

$C_{d,mean}$	=	mean blade drag coefficient
CP	=	collective pitch, °
D_r	=	wind axis rotor drag, lb_f
F_n	=	thrust produced by the rotors (total), lb_f
K_p	=	proportional control gain
K_i	=	integral control gain
K_{it}	=	zero steady-state torque command integral control gain
N_g	=	gas generator speed, rpm
N_p	=	power turbine speed, rpm
N_r	=	rotor speed, rpm
P_{EMg}	=	power applied by the electric machine on the gas generator spool, hp
P_{EMp}	=	power applied by the electric machine on the power turbine, hp
P_{EMr}	=	power applied by the electric machine on the rotor, hp
P_i	=	induced power, hp
P_{ideal}	=	ideal induced power, hp
P_o	=	profile power, hp
P_p	=	parasitic power, hp
P_{s3}	=	static compressor discharge pressure, psi
P_{sh}	=	rotor shaft power (single rotor), hp

¹ Research Engineer, Intelligent Control & Autonomy Branch, AIAA member.

² Research Engineer, Intelligent Control & Autonomy Branch, Senior AIAA member.

$PSFC$	=	power specific fuel consumption, hp/(lb _m /hr)
N	=	generic shaft speed
N_{sp}	=	generic shaft speed set-point
SM	=	compressor stall margin, %
SOC	=	state of charge, %
T_d	=	turbine inlet temperature, °R
$TSFC$	=	thrust specific fuel consumption, lb _f /(lb _m /hr)
V	=	freestream airspeed
V_{ideal}	=	ideal induced velocity, ft/s
W_c	=	corrected mass flow rate, lb _m /s
w_f	=	fuel flow rate, lb _m /s
$w_{f,cmd}$	=	fuel flow rate command, lb _m /s
$w_{f,max}$	=	fuel flow rate at maximum power, lb _m /s
$w_{f,min}$	=	fuel flow rate at idle, lb _m /s
$w_{f,norm}$	=	normalized fuel flow rate
κ	=	induced power factor
σ	=	thrust-weighted solidity
τ_{EMg}	=	torque applied by the electric machine on the gas generator spool
τ_{EMp}	=	torque applied by the electric machine on the power turbine
τ_{EMr}	=	torque applied by the electric machine on the rotor
$\tau_{EM,c}$	=	generic torque command

II. Introduction

Turbine Electrified Energy Management (TEEM) is an operability control concept for electrified gas turbine engines. TEEM leverages electrical components present in new propulsion system concepts, specifically those integrated with a gas turbine engine. Most notably, electric machines (EMs) (motors/generators) and energy storage devices (ESDs) are treated as additional actuators in the propulsion system to modify the system's behavior. Combined with this control strategy, the electrical components are used to improve the operability of the turbomachinery and enable new capabilities for the propulsion system and aircraft. Operability benefits shown in this study, can be leveraged to improve systems safety and or performance. Operability requirements constrain the design space of the engine, and so improved operability is expected to enable design solutions that result in a more efficient and lighter-weight engine. In addition, the electrical system provides a means for more direct benefits such as the reduction of engine bleeds.

TEEM has been the topic of prior research efforts [1,2,3]. The TEEM concept was first applied in Ref. [1] to the Parallel Hybrid Electric hFan concept described in Ref. [4]. The hybrid electric concept uses a motor on the low pressure spool of a turbofan engine to augment thrust. The additional power is provided to the motors by batteries housed in under-wing pods. The propulsion system is meant to power the single-aisle SUGAR-Volt airframe [4]. The study established a method by which power management on the spools of a gas turbine engine can be used to prevent compressor stall during transients. Reference [1] outlined the use of electric machines to extract/apply power from/to the engine spools in order to reduce or even eliminate engine bleeds meant to maintain compressor stability, particularly at low power settings. The study also found that the EM and ESD requirements for applying TEEM were reasonable, when considering that the requirements can be met by the baseline propulsion system concept's electrical components. References [2] and [3] applied TEEM to a standalone engine to explore the feasibility of its adoption in the near term to a more electric engine with the objective that it could accelerate the path toward more electrified propulsion systems. Reference [2] provided simulation results of a high level control strategy for implementing TEEM that substantially improved transient operability and addressed the in-flight maintenance of ESD charge to help reduce their size. The control strategy for in-flight charging used the engine actuators (a variable bleed valve and variable area fan nozzle) in coordination with the off-nominal power extraction associated with charging to maintain the same operability margins as the baseline engine. This illustrated the possibility of optimizing actuator usage and implementing reversionary control modes should any of the actuators fail or be limited to partial use. This paper also conjectured about the possibility of other benefits such as assisting the high pressure spool with power in put during ground operations to reduce fuel burn while simultaneously improving LPC operability at low power conditions. Given the improvement in LPC operability, the need for compressor bleeds are reduced. Reference [3] presented an analysis of electrical system requirements for implementing TEEM on the same gas turbine engine considered in [2].

Those results suggested that applying TEEM to a conventional engine is within the realm of possibility for early adoption toward the electrification of aircraft propulsion systems.

The studies mentioned above were geared toward large engines on large single-aisle commercial transports. In this paper, TEEM is applied to the propulsion system of a conceptual 15 passenger turbo-electric tilt-wing vehicle. The conceptual Tilt-Wing vehicle is depicted in Fig. 1. While it has been shown in simulation that TEEM has a substantial impact on large engines, the impact is expected to dwindle for smaller engines due to the reduced inertia of the engine shafts that tend to be associated with better transient operability characteristics. This would shrink the potential impact that TEEM has on transient operability, which is expected to produce a significant portion of the control strategy's benefit. The focus of this paper is to determine the impact of TEEM for a substantially smaller propulsion system. In this case a ~4000 hp turboshaft engine. Not only is the engine smaller, but the Tilt-Wing propulsion system concept has a number of other key differences compared to the propulsion systems studied previously. This is the first turboshaft engine using the TEEM control approach. It is also the first single-spool gas generator, and the first to have a power turbine. In addition, it is the first vehicle considered that uses the gas turbine for power generation to drive external propulsors. This allows the TEEM control approach access to an expanded electrical system to impact components outside of the engine. Given the unique operation of the Tilt-Wing vehicle, there was also interest in exploring how TEEM and its electrical hardware could be used to enhance the overall vehicle performance and capabilities.

The rest of this paper is organized as follows. Section III introduces the Tilt-Wing vehicle and describes the propulsion system. Section IV describes the propulsion system model and Section V describes its baseline controller.

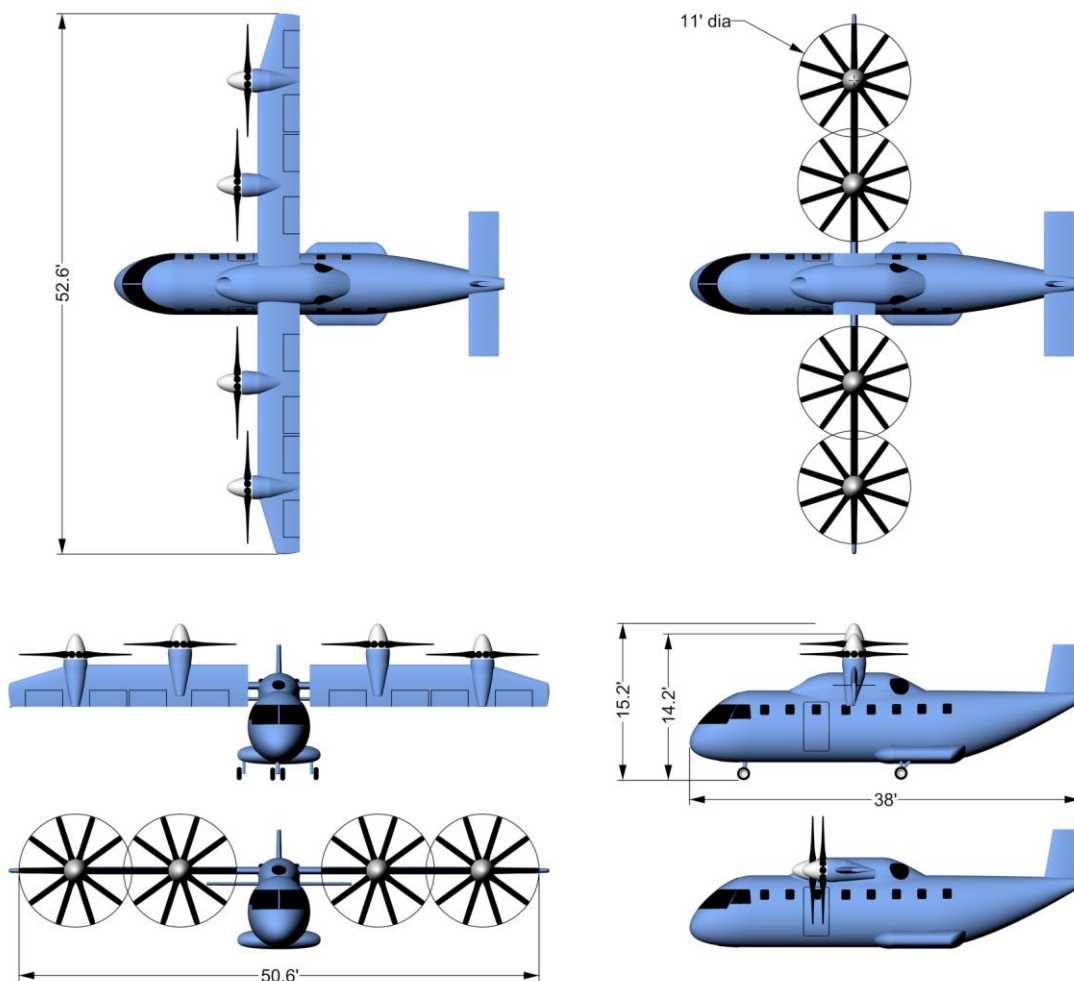


Figure 1. Notional representation of the NASA Tilt-Wing concept vehicle [5].

Section VI describes the power/energy management control strategy. Section VII presents and discusses simulation results and Section VIII offers some concluding remarks.

III. The Tilt-Wing Propulsion System

The propulsion system investigated here is based upon the NASA Tilt-Wing concept vehicle [5]. While some inconsistencies may exist with the official concept, it shares many commonalities and can be viewed as being a very close variant of the NASA concept. Specifically, there are small discrepancies in model parameters, including electrical component efficiencies that demanded a slightly larger turboshaft engine. In addition, there is the potential that the rotor model and its parameters are not identical. Some features of the Tilt-Wing, such as its rotor speed set-point schedule, were not previously defined, leading to potential departures from the official concept when defined for this study.

The Tilt-Wing concept vehicle is a short-range commercial transport capable of carrying 15 passengers. The vehicle propulsion system is represented as a block diagram in Fig. 2. The pictographs used in Fig. 2 follow the AIAA standard proposed in [6]. The vehicle is propelled by 4 identical wing-mounted rotors that are each driven by an electric motor. The electric motors derive their power from a single gas-driven turboshaft engine via a generator attached to the power turbine of the turboshaft engine. The power turbine is denoted by PT in Fig. 2. Electrical power generated by the turboshaft is assumed to be transmitted through a rectifier, DC-DC converter, various cables, and a motor controller prior to being applied by each motor to the rotors. Gearboxes are present between each of the electric machines and the shafts they seek to affect. A battery is also present in the system but it is only intended for emergency use in the case of an engine failure. The battery is sized for 2 min of hover to allow time for the aircraft to safely land [5]. To improve the battery's energy density it is only designed for a single-use.

The Tilt-Wing vehicle has a total range of 400 nm. As the name implies, the wing can rotate between 0° (aligned with the fuselage in the horizontal position) and 90° (in the vertical position). Since the rotors are fixed to the wings, this also implies that the rotors will rotate with the wings. The Tilt-Wing configuration allows the vehicle to take-off and land vertically to eliminate the need for a runway, and it can fly efficiently at relatively fast speeds compared to other vertical lift vehicles such as helicopters.

The turboshaft is capable of generating roughly 4000 hp through a generator connected to the power turbine. Each of the 4 rotors has 10 blades and spans a diameter of 11 ft. The thrust generated by the rotors is controlled by the collective pitch (CP) of the blades. In theory, the rotors will also have cyclic pitch control to maneuver between hover and forward flight.

The Tilt-Wing propulsion system requires a few modifications to facilitate the TEEM application. This includes the presence of an electric machine on the gas generator of the turboshaft engine. While such an EM is not mentioned in the baseline concept, the addition of an EM may not be necessary. This is because the engine will require such a device to start the engine that could be leveraged for the TEEM control strategy. However, the TEEM

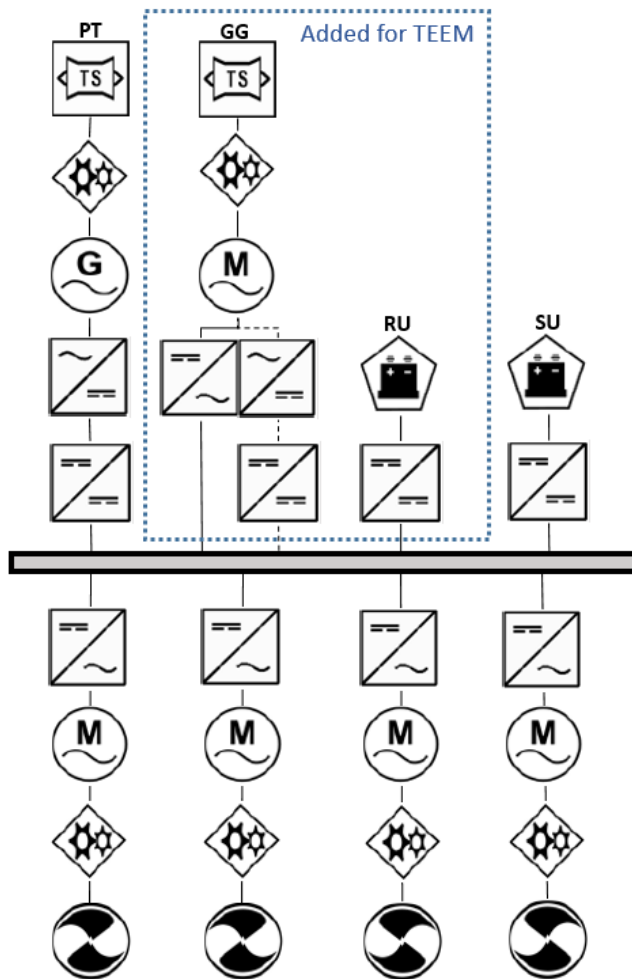


Figure 2. Tilt-Wing propulsion system block diagram. Components inside the dashed blue line are added for TEEM.

application may influence its power requirement. Therefore, the application of TEEM will at worst require a larger electric starter motor. In addition, TEEM requires a small amount of re-useable energy storage. This means that re-usable energy storage must be added to the vehicle or a portion of re-usable energy storage that is already present in the system should be made available for TEEM. The modified propulsion system is represented in Fig. 2, with inclusion of the components within the blue dotted box. “GG” signifies the gas generator of the turboshaft engine. “RU” signifies re-usable energy storage as opposed to the single-use battery that is included in the baseline concept. The re-usable energy storage is represented with a battery pictograph. However, this should be thought of as a generic energy storage device.

IV. Propulsion System Model

The Tilt-Wing propulsion system is modeled in the MATLAB/Simulink® coding environment. The Toolbox for Modeling and Analysis of Thermodynamic Systems (T-MATS) [7] is used to model the turboshaft engine. The rotor model is coded in MATLAB/Simulink based on theory applied by the NASA Design and Analysis of RotorCraft (NDARC) software. The electrical system was modeled simplistically by neglecting electrical system dynamics and applying bulk efficiencies for each of the electrical components. The following sub-sections provide more details about the turboshaft, rotor, and electrical system models. These models were integrated to obtain the overall Tilt-Wing propulsion system model.

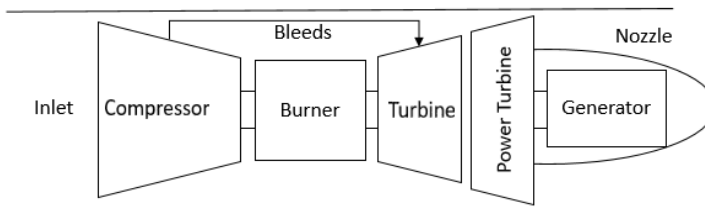


Figure 3. Turboshaft engine schematic for the baseline Tilt-Wing concept vehicle.

A. Turboshaft

T-MATS is a modular modeling tool that is well-suited for constructing dynamic models of gas turbine engines. T-MATS provides tools for modeling the thermodynamic processes that occur within a gas turbine engine. It utilizes performance maps to model the off-design operation of turbomachinery components (e.g. compressors and turbines) and has the ability to include shaft dynamics. T-MATS uses an iterative solver to satisfy conservation equations. The model is zero-dimensional (0-D), which combines bulk component level models to create an overall system model.

The turboshaft engine is represented in Fig. 3. The gas generator consists of an inlet, a compressor, a burner, and a turbine. Bleeds are present in the compressor to cool the turbine. A free power turbine is present downstream of the gas generator turbine and it is followed by a nozzle. Generic performance maps were used to model off-nominal operation of the engine. Those maps along with their design point are shown in Figs. 4-6. PR is the pressure ratio across the component and W_c is corrected mass flow rate. The design point was at a hover condition with an altitude of 5000 ft above sea level and an ambient temperature of 37 °F above standard atmosphere (96 °F at sea level). Table 1 provides key modeling parameters, design point scaling parameters, and performance metrics.

An equivalent Numerical Propulsion System Simulation (NPSS) steady-state model was developed prior to the T-MATS dynamic model. NPSS is a NASA developed industry standard

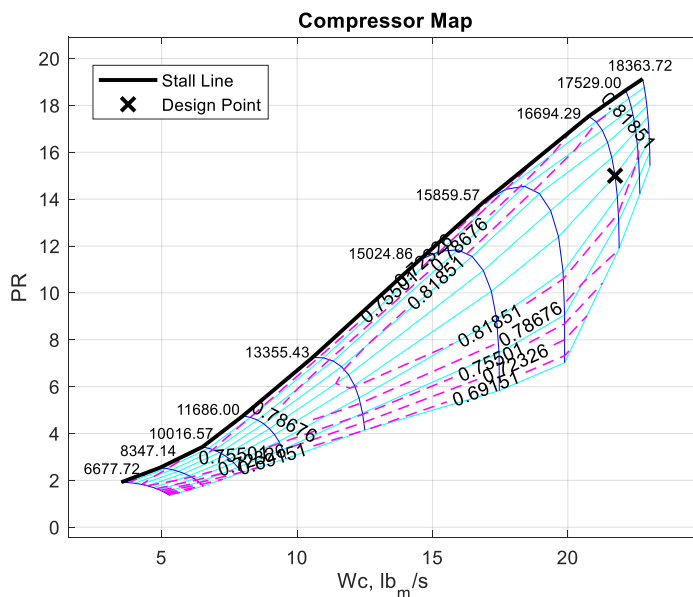


Figure 4. Compressor map with its design point. The blue lines are constant speed lines, the dashed magenta lines are constant efficiency lines, and the cyan lines are referred to as R-lines.

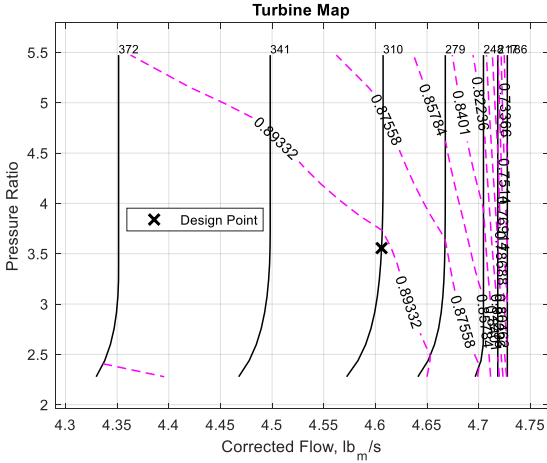


Figure 5. Gas generator turbine map. The black lines are constant corrected speed lines and the dashed magenta lines are constant efficiency contours.

cycle design and analysis tool. NPSS was used here to perform a weight analysis in order to get approximations for the inertias of the gas generator spool and power turbine that are required to simulate shaft dynamics. This was done through the use of an NPSS Weight Analysis Turbine Engine (WATE) [8] model. The inertias were estimated to be 0.35 slug-ft² and 0.11 slug-ft² for the gas generator spool and power turbine respectively.

B. Rotors

NDARC is a conceptual design and analysis code for performance analysis and sizing of new rotorcraft concepts. It has a modular architecture that allows the user to model and size various rotorcraft components that eventually results in a vehicle level model. In this instance, the rotors were the only components of interest from the perspective of modeling the propulsion system.

NDARC is a fairly complex modeling tool not conducive for integration with the other coding environments discussed. Furthermore, with the focus on the propulsion system, it was unnecessary to include extraneous systems captured by NDARC. Therefore, the rotors were modeled in MATLAB/Simulink based upon the theory used by NDARC [9,10].

The need for the rotor model is to produce a representative thrust and shaft power output that is fed to the rest of the propulsion system to simulate the impact on the turbomachinery. Thrust and shaft power computations are performed separately but are coupled, thus requiring iteration to reach a solution. Details are provided in [9] but the high level approach is outlined here.

The rotor power is broken into three components: induced power, profile power, and parasitic power. Induced power is computed from ideal power using an energy performance method. The induced power P_i is computed with Eq. (1) where κ can be thought of as an efficiency, P_{ideal} is the ideal induced power, v_{ideal} is the ideal induced velocity, and F_n is the thrust generated by the rotor.

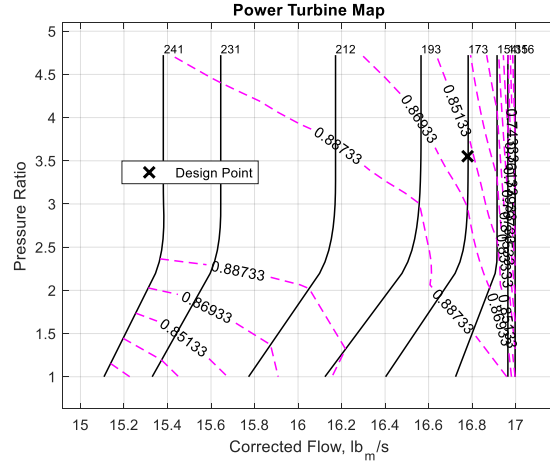


Figure 6. Power turbine map. The black lines are constant corrected speed lines and the dashed magenta lines are constant efficiency contours.

Table 1. Engine design point parameters and performance

		Parameter	Value
Compressor	Speed		17000 rpm
	Efficiency		0.8377
	Pressure Ratio		15
	R-line		2.0
	Discharge bleed fractions for turbine cooling (turbine inlet, turbine exit)		0.0901, 0.0916
	R-line		2.0
Burner	Lower Heating Value		18500 Btu/lb _m
	Pressure Drop		3%
Turbine	Speed		17000 rpm
	Efficiency		0.8963
	Map Pressure Ratio		5
Power Turbine	Speed		8000
	Efficiency		0.8665
	Map Pressure Ratio		5
Nozzle	Design Flow Rate		18.19 lb _m /s
	Velocity Coefficient		0.99
	Throat Area		102.3 in ²
Overall Performance	Power Extraction		3250 hp
	Fuel Burn		0.4221 lb _m /s

$$P_i = \kappa P_{ideal} = \kappa F_n v_{ideal} \quad (1)$$

Calculation of κ relies on empirical models. In this case the parameters are defined based on higher-fidelity simulations performed with the NASA-developed Comprehensive Analytical Model of Rotorcraft Aerodynamics and Dynamics (CAMRAD) II [11] software. The profile power P_o is computed from the mean blade drag coefficient:

$$P_o = \frac{\sigma}{8} c_{d,mean} F_P \quad (2)$$

where σ is the thrust-weighted solidity, $c_{d,mean}$ is the mean blade drag coefficient, and F_P is a factor that accounts for the increase of the blade section velocity with rotor edgewise and axial speed. The mean blade drag coefficient is estimated as a function of blade loading C_T/σ where C_T is the thrust coefficient. The mean blade drag coefficient attempts to address both helicopter and propeller flight and introduces a means to include stall and compressibility effects. This mostly boils down to empirically tuned model parameters based on results from CAMRAD II. The parasitic power P_p is obtained from the drag force.

$$P_p = D_r V \quad (3)$$

In Eq. (3), D_r is the wind axis drag on the rotor and V is the freestream velocity magnitude. The rotor drag is calculated while determining the rotor forces and the air speed is known.

Blade element theory is the basis for determining the flapping and coning angles of the rotor blades as well as the thrust. Blade element theory divides the rotor into several independent sections along its length. The lift and drag forces generated by each blade section are used to determine the rotor forces, including thrust. The section forces are integrated over the length of the blade and averaged over a single revolution to determine the overall forces produced by the rotor. The blade section aerodynamics are modeled with a lift equation that varies linearly with respect to angle of attack, and the mean drag coefficient from the profile power calculation is used for the drag analysis. The cyclic pitch and flapping relationship is defined by the rotor flap dynamics equations. Thrust and flapping equations of motion must be satisfied. The thrust and flapping equations are accompanied by an equation comparing the previous coning angle guess to the current guess. The solver independents include the blade loading, longitudinal and lateral flapping angles, and the coning angle. A Newton-Raphson solver was used to obtain a solution at each time-step of the simulation. The iterative solver is wrapped by code that applies dynamics to the rotor shaft. The inertia of the rotor was readily approximated from the rotor lock number and other known quantities from the NDARC model. Collective pitch as well as longitudinal and lateral cyclic pitch are prescribed inputs to the rotor model. Keep in mind that the goal of the study is to assess power management techniques. Given that this study is not concerned with flight dynamics and control, the cyclic pitch values were fixed at zero through much of the studies. While cyclic pitch controls would be necessary for modeling the transition between hover and forward flight, this segment of flight was not of concern for control development for this study. Thus the inclusion of cyclic pitch controls was unnecessary for this study. Collective pitch was controlled to produce the desired rotor shaft power and corresponding thrust. This enabled the rotor model to supply the rest of the propulsion system model with shaft power demands without cyclic pitch controls.

Since the rotors are assumed to be identical and operate in unison, only one rotor is modeled in Simulink. Inputs and outputs to the rotor model are simply adjusted by a factor of 1/4 or 4 where applicable. The Simulink rotor model was compared against steady-state outputs from the NDARC model provided in Table 2. The comparison of the thrust and shaft power results at hover and cruise for an altitude of 5,000 ft were in agreement to within one half percent.

Table 2. Comparison of Simulink Model to NDARC. Results are for a single rotor.

	NDARC	Simulink Model	Percent Error
Hover Shaft Power	704.2 hp	702.0 hp	0.31%
Hover Thrust	3463.6 lb _f	3463.2 lb _f	0.01%
Cruise Shaft Power	244.8 hp	244.7 hp	0.04%
Cruise Thrust	325.8 lb _f	325.8 lb _f	0.00%

C. Electrical System and Gearboxes

The electrical system consists of a generator, a rectifier, a DC-DC converter, 4 motors, and a motor controller for each motor. The generator is roughly 3600 hp and the rotor motors are roughly 800 hp. Since only one of the rotors is modeled, only a single string of the motor controller and motors is considered in the model. The power downstream of the DC-DC converter is simply divided by 4. The generator and motors are each assigned an efficiency of 97%. The rectifier, motor controllers, and DC-DC converters are each assigned an efficiency of 98.6%. The generator is connected to the power turbine through a gearbox and the motors are connected to the rotor shafts through a gearbox. The gearbox efficiency is 98%. The application of TEEM required consideration of an electric machine connected to the gas generator and usage of energy storage. The gas generator electric machine efficiency is the same as the electric machines on the power turbine and rotors. The electric machine is connected to the gas generator through a gearbox which has an efficiency of 98%. Energy storage is included to meet the demands of the electrical machines. Any non-zero summation of power on the electrical bus is supplied or absorbed by the ESD and that power is integrated to track the change in ESD energy and its state of charge (*SOC*). For the purposes of this study, the ESD assumes a useful energy capacity of 0.7 kW-hr.

D. Flight Dynamic Model

A simple flight dynamic model was created to study rotor shaft power requirements throughout the transition from hover to forward flight or visa versa. This was to understand if there are flight conditions in which the turboshaft engine may be undersized, leading to a potential application of thrust augmentation through the power system. The flight dynamics model was integrated with the rotor model to provide trim conditions of the aircraft at numerous angles of the tilt-wing between 90° and 0°. The flight dynamic model consists of simple aerodynamic equations for calculating lift and drag for each of the vehicle components (wing, fuselage, horizontal tail, etc.). Moments about the center of gravity were also calculated. Dynamic equations governing the motion of the aircraft were set to zero to derive the trim conditions. Forward/backward, and side-to-side motion were considered along with pitching motion. The independent variables included the thrust, velocity, and horizontal tail pitch or cyclic pitch of the rotor. The vehicle weight and the computed aerodynamic forces were used to determine the speed and orientation of the vehicle. The modeling approach and parameter values were gleaned from [9]. Note that the flight dynamic model is only applicable to this specific study, which will be presented at the end of the results section.

V. Baseline Control

The Tilt-Wing propulsion system must provide the thrust or shaft power required to achieve the desired air speed. Simultaneously, the power turbine speed and rotor speeds are tightly regulated. Due to the coupled nature of the propulsion system along with multiple control objectives, a multi-variable control approach is applied to the Tilt-Wing propulsion system. Specifically, a gain-scheduled Linear Quadratic Regulator (LQR) design with integral action for reference tracking is employed. The controller regulates the speed of the power turbine at 8,000 rpm across all operating conditions. The rotor speed set-point is shown in Fig. 7. It is a function of airspeed with the form of a logistic equation. Finally, the rotor shaft power is a function of Mach number, altitude, and power level (*PL*). The *PL* ranges from 0 to 100 and varies linearly with thrust where 0 corresponds to idle and 100 corresponds to maximum power or thrust. The control inputs consist of the turboshaft fuel flow w_f , the torque applied to the power turbine by the generator for power extraction τ_{EMp} , and the collective pitch (*CP*) of the rotors. As discussed, cyclic pitch is not considered here as flight dynamics are not presently of concern and collective pitch is sufficient to investigate power transients. Limit logic is applied within the shaft power set-point controller to prevent the turboshaft engine from violating various operability limits including over-speed of the engine shafts, over-temperature at the compressor exit and turbine inlet, maximum and minimum static pressure at the exit of the compressor, and acceleration and deceleration limits. The propulsion system model and baseline controller exhibit expected transient responses. The target rotor shaft power is reached within 5 s as required by [12] and the rotor speed regulation is reasonable, maintaining the rotor speed within 3.5% of the set-point value. In Fig. 8 the control inputs are shown

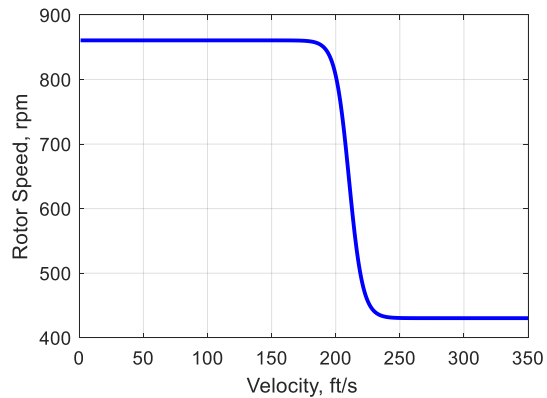


Figure 7. Rotor speed set-point schedule.

and in Fig. 9a-9d the closed-loop system behavior for a burst and chop transient at static conditions on a hot day (37 °F above standard atmosphere) at an altitude of 5,000 ft are shown.

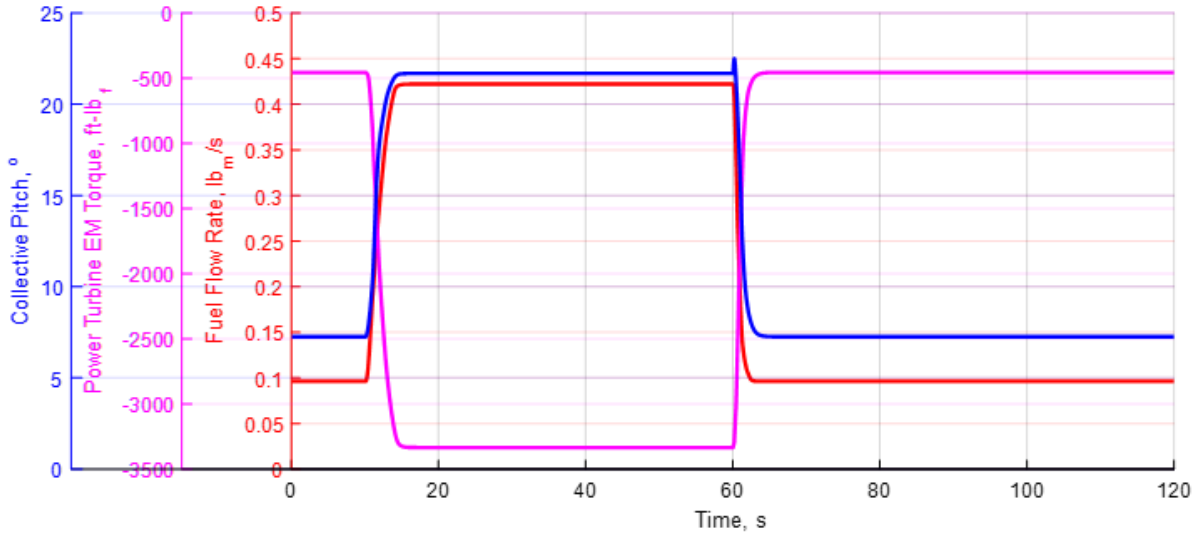


Figure 8. Control inputs for a burst and chop power transient scenario.

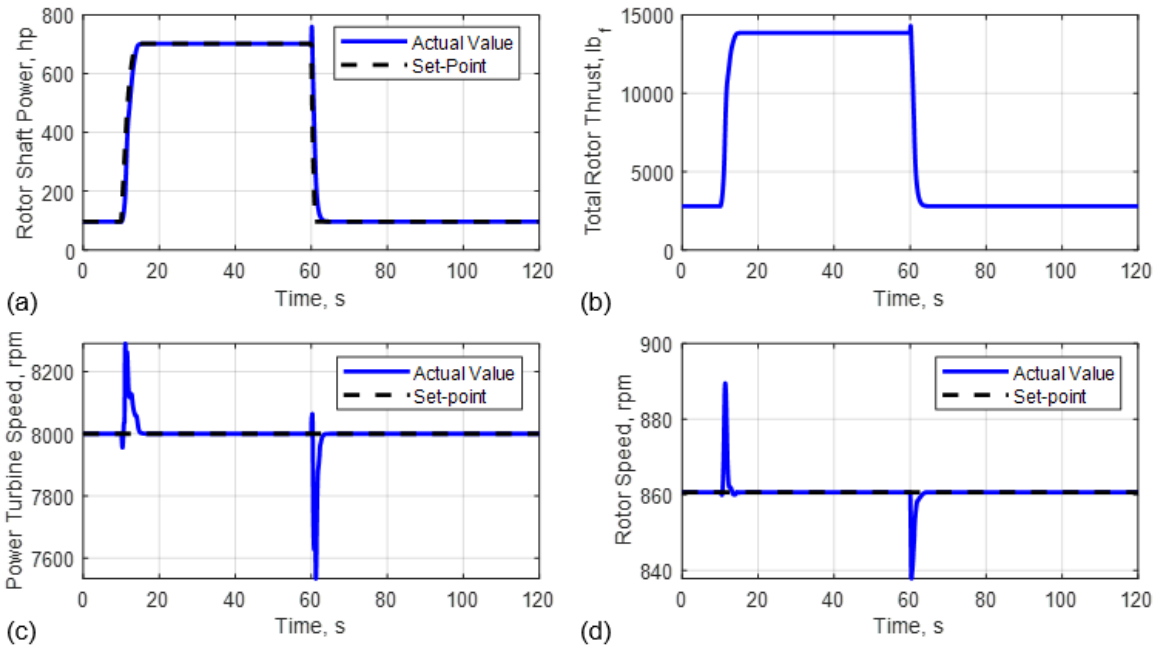


Figure 9. Response of the baseline system to a burst and chop power profile.

VI. TEEM Control

Applications of power/energy management has numerous applications including the use of persistent power injection to enable a smaller engine sized for the bulk of the mission or persistent power extraction to increase power and thrust of the rotors or to drive additional propulsors, etc. However, these options depart significantly from the baseline concept and it becomes an exercise of architecture selection and aircraft design rather than power/energy management and control. Therefore, the focus here is placed on how power/energy is managed on the baseline vehicle with no additional equipment beyond what is present to implement TEEM transient control. The strategies investigated

utilized power collected during transients to temporarily reduce fuel burn, and utilize the energy storage to temporarily supplement power production from the turboshaft to increase thrust. This allows the vehicle to access additional thrust during an emergency situation, increase take-off weight, and/or enable the aircraft to hover at higher altitudes.

In the prior studies documented in [1–3], all of the thrust was produced by the gas turbine engine(s), with the exception of the hFan, where some of the power to drive the fan was sourced by a battery-driven electric motor. Power/thrust management only required control of the fan speed. Even with the hFan concept, this was not much of a departure from a conventional engine in-terms of the means of thrust production. The only electric machines in the propulsion system were those integrated with the engine. The Tilt-Wing propulsion system has some key differences with the prior studies that caused the transient TEEM control strategy to be re-evaluated. Mainly, the Tilt-Wing has electric machines that drive propulsors external to the engine, and the controller is posed with multiple objectives.

The TEEM controller is designed independently from the baseline power management controller described in the previous section. The transient speed control architecture consists of three proportional integral (PI) controllers with integral wind-up protection: the gas generator motor, the rotor electric machines, and the power turbine. The controllers command off-nominal torques to closely match the steady-state shaft speed conditions. The goal is to suppress excursions of the compressor operating point away from its steady-state operating line. The gas generator set-point speed is determined from a schedule based on the Mach number, altitude, and normalized fuel flow $w_{f,norm}$.

$$w_{f,norm} = \min\left(1, \max\left(0, \frac{w_{f,cmd} - w_{f,min}}{w_{f,max} - w_{f,min}}\right)\right) \quad (4)$$

Equation (4) forces a value of $w_{f,norm}$ between 0 and 1. A value of 0 corresponds to idle and 1 to maximum power. In Eq. (4), $w_{f,min}$ and $w_{f,max}$ are the minimum and maximum fuel flow rates for a given altitude and Mach number, and $w_{f,cmd}$ is the fuel flow commanded by the controller.

Included in the controller is logic to sense when a transient is occurring. This information is used to activate or de-activate the transient TEEM controller for the gas generator electric machine. If the controller were to remain active during steady-state it could result in continued power extraction or injection that would alter steady-state performance and deplete or over-charge the ESD(s). This issue results from the potential that the gas generator set-point speed may not match its natural speed due to engine degradation among various other factors. The rotor and power turbine electric machine controllers do not require such logic because their set-points coincide with the nominal controller set-points and they contain an extra integral term in their control laws to assure electric machine torques are driven to zero at steady-state as shown in Eq. (5). K_p is the proportional control gain, K_i is the integral control gain, K_{it} is the integral control gain for enforcing a zero steady-state torque command, N is the speed of the rotor or power turbine, N_{sp} is the set-point speed, Δt is the sampling time of the discrete controller, and $\tau_{EM,c}$ is the torque command.

$$\tau_{EM,c} = K_p(N_{sp} - N) + K_i(N_{sp} - N)\frac{\Delta t}{z - 1} + K_{it}\tau_{EM,c}\frac{\Delta t}{z - 1} \quad (5)$$

Transients are sensed by observing the error between the set-point and measured/calculated rotor shaft power. If the error is greater than the prescribed threshold then the transient TEEM control logic for the gas generator electric machine is activated. To promote a smooth transition from TEEM transient control to “steady-state” operation, the torque commands produced by the PI controllers are multiplied by a taper factor that ranges between 0 and 1. The taper factor is prescribed by a logistic function with respect to the rotor shaft power error. For most values of shaft power error, the taper factor is 1, but at very low error values it transitions smoothly to a value of 0.

The portion of energy storage utilized by the transient TEEM control strategy is proposed to be regulated at an intermediate *SOC* so that power can be supplied or absorbed at any time. In this case, the nominal *SOC* was chosen to be 50%. During early simulations studies with the TEEM transient controller, it was observed that transients often result in a net power extraction. This influenced the decision to maintain a nominal *SOC* at an intermediate value. It also posed the question of what to do with the excess energy. The solution pursued here is to apply the excess energy to the rotors proceeding each transient, resulting in a temporary reduction in fuel consumption until the energy collected during the transient is dissipated. In this case the ESD dissipates the excess energy at a rate of 10 hp and that value tapers to 0 as the nominal *SOC* is approached. In the case that the ESD discharges below its nominal *SOC*, a charging schedule is present that will extract a small amount of additional power from the power turbine to charge the ESD. In this case, the additional power extraction is 50 hp and tapers to zero as the nominal *SOC* is approached. In all cases, power input or extraction commands are converted to torque commands using the sensed speeds of the relevant shafts.

The rotor shaft power set-point command is modified to enable a request for additional power. The power level (PL) command from the pilot is extended to a maximum value of 107 which roughly translates to a 7% increase in the thrust achieved at a power setting of 100. The additional power required to fulfill the request is supplied by the ESD to the rotor motors. The power could come from the single-use battery or the re-usable energy storage depending on the scenario. It may not be necessary to increase the size of the electric machines to apply the additional power because EMs can typically supply more power than their continuous rating for brief periods of time. In other words, if it is only used for a quick evasive maneuver or over the course of a short duration hover with an increased payload or at a higher than typical altitude, then the baseline motors may be sufficient. The additional power request is added to the nominal shaft power request determined by the baseline set-point controller. The amount of additional power increases linearly with PL over 100. A rate limit is applied to any PL command that exceeds 100 in order to prevent the power from being instantaneously applied to the detriment of the rotor's operability. The power command is converted to a torque command using the sensed value of the rotor speed. The turboshaft engine will supply as much of the power as it can until it hits an operating limit, after which it will ride that limit. The deficit in power needed to drive the rotors is supplied by the ESD(s).

VII. Simulation Results

Results are presented to illustrate the enhancements made by the power management and control strategy. Much of the results are for a burst and chop power transient at sea level static conditions. Fig. 10 shows the change in power level with respect to time. In Fig. 11a and 11b the response of the power turbine and rotor speed respectively is shown. The results indicate that TEEM achieves tighter regulation of these speeds. Tight regulation of the rotor and power turbine speed is beneficial because it helps to alleviate pilot workload, prevents the shafts from over-speeding, and keeps the turbine and rotor blades operating closer to their design incidence angles. The stall margin variation throughout the power maneuvers is shown in Fig. 12. During the acceleration transient, a $\sim 3.75\%$ improvement in stall margin is observed. The impact on compressor operability is provided with respect to the compressor performance map in Fig. 13. The result indicates suppression of the operating point's tendency to move toward the stall line during the transient. The power supplied to each electric machine is shown in Fig. 14. The gas generator EM applies approximately 175 hp. The off-nominal power turbine EM power approaches 500 hp but the maximum overall power extraction is only 100 hp above the baseline maximum power extraction, which should be well within the capability of the EM for short duration transitions. The off-nominal rotor EM power approaches 50 hp, which is also expected to be within the capability of the EM for short durations. Thus, the gas generator EM, the ESD(s), and their supporting equipment are the only

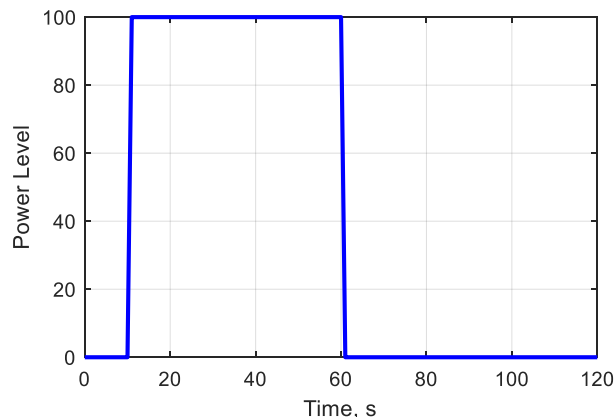


Figure 10. Power level command for a burst and chop power transient.

The power supplied to each electric machine is shown in Fig. 14. The gas generator EM applies approximately 175 hp. The off-nominal power turbine EM power approaches 500 hp but the maximum overall power extraction is only 100 hp above the baseline maximum power extraction, which should be well within the capability of the EM for short duration transitions. The off-nominal rotor EM power approaches 50 hp, which is also expected to be within the capability of the EM for short durations. Thus, the gas generator EM, the ESD(s), and their supporting equipment are the only

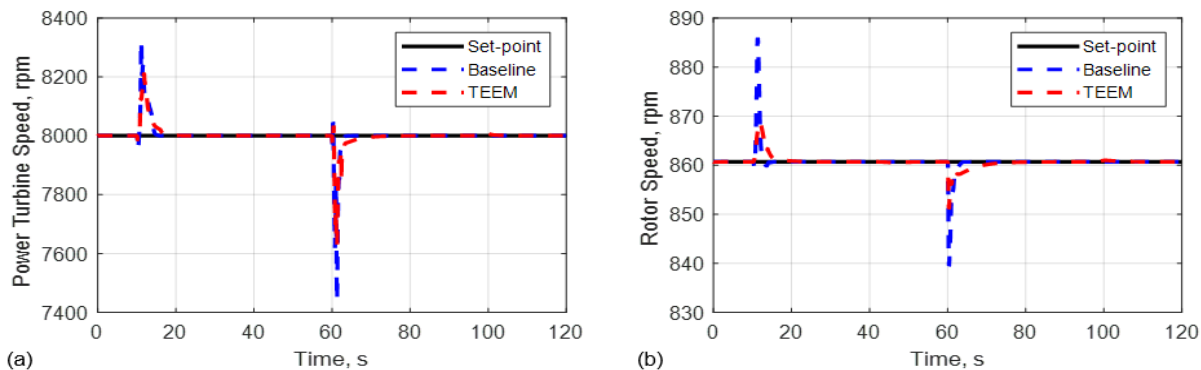


Figure 11. Shaft speed regulation for a burst and chop power transient at sea level static conditions.

components that would possibly need to buy their way into the propulsion system. Note that it is expected that a gas generator EM will be included for the purpose of engine starting and aircraft power extraction. Furthermore, ESDs could be onboard to support engine start-up and to power preflight systems, among other potential uses. Therefore, the baseline Tilt-Wing vehicle is expected to have all or a significant portion of the infrastructure necessary to support TEEM. The ESD power, energy, and state of charge are shown in Fig. 15. The ESD is sized sufficiently to handle this extreme transient scenario. It is also able to re-charge or dissipate excess energy to return to its nominal SOC within ~40 s and there is potential to reduce that timespan.

An interesting observation is that the power injection/extraction trends are opposite compared to the applications in [1] and [2]. During accelerations, power would typically be supplied by the ESD to speed up the compressor. While power tends to be injected into the gas generator via its electric machine to speed it up during accelerations, power tends to be extracted from the rotors and power turbine to prevent over-speeding. The explanation for this is that the multi-variable controller tends to lead with fuel flow followed by generator torque and then collective pitch. This allows the engine to stay ahead of the rotor demand to avoid droop in the power turbine speed and rotor speed. This ends up being advantageous, because it offsets the power needed from the ESD during the transient. In fact, the end result is a net power extraction. Similarly during deceleration, power was extracted from the compressor in previous studies. While this is the case here as well, power is also added to the rotors and power turbine to keep their speeds tightly regulated. This results in a net power injection. A similar explanation is applicable here, as that described for the acceleration case, and this too ends up being beneficial as the power extraction from the gas generator offsets the overall power injection needed from the ESD. The Thrust Specific Fuel Consumption (*TSFC*) and Power Specific Fuel Consumption (*PSFC*) following the acceleration transient is reduced by ~1.3%. Of course, there is a temporary increase in fuel consumption after deceleration transients. In this particular simulation scenario the *TSFC* is increased by ~5% during the short charging period. While the duration of charge is similar to the duration of power injection following the acceleration transient, the fuel flow rate during the charging period is ~25% of that occurring at the end of the acceleration transient. For the duration of the simulation, the engine burned 0.3% less fuel with TEEM, indicating a slight fuel burn benefit when considering acceleration and deceleration power transients of similar severity. It is also note-worthy that the need to reduce power quickly is less of a concern than increasing power quickly and deceleration transients tend to be more gradual. Therefore, it is expected that a net power extraction will occur throughout a practical mission, resulting in a slight fuel burn reduction.

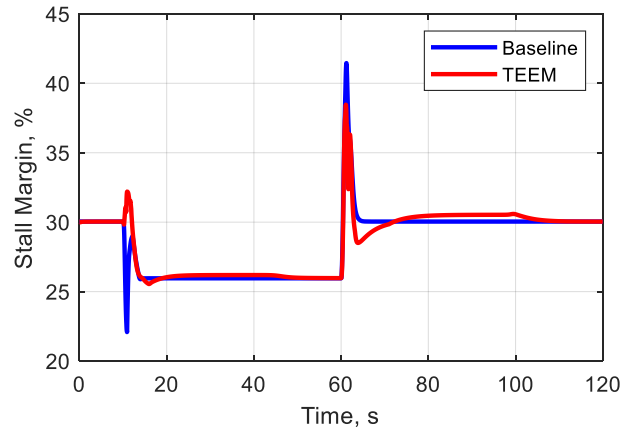


Figure 12. Stall margin response for the baseline and TEEM control strategy.

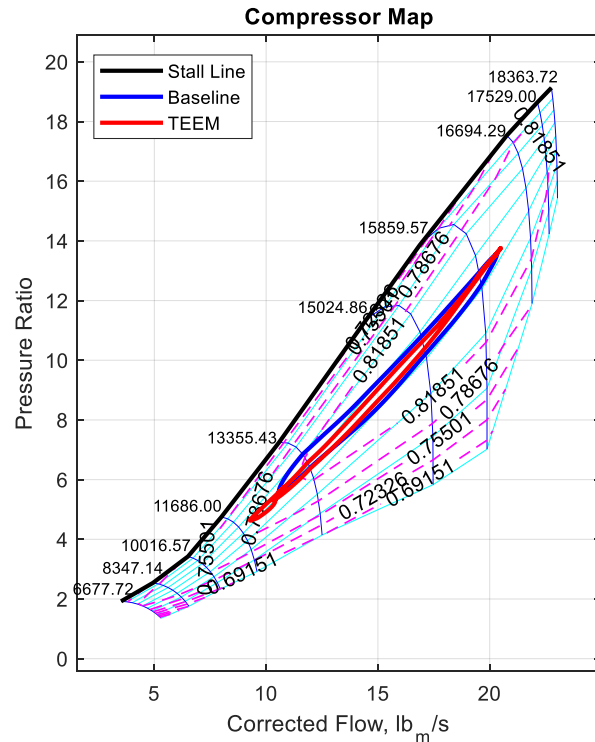


Figure 13. Compressor map with operating point deviations during a burst and chop transient.

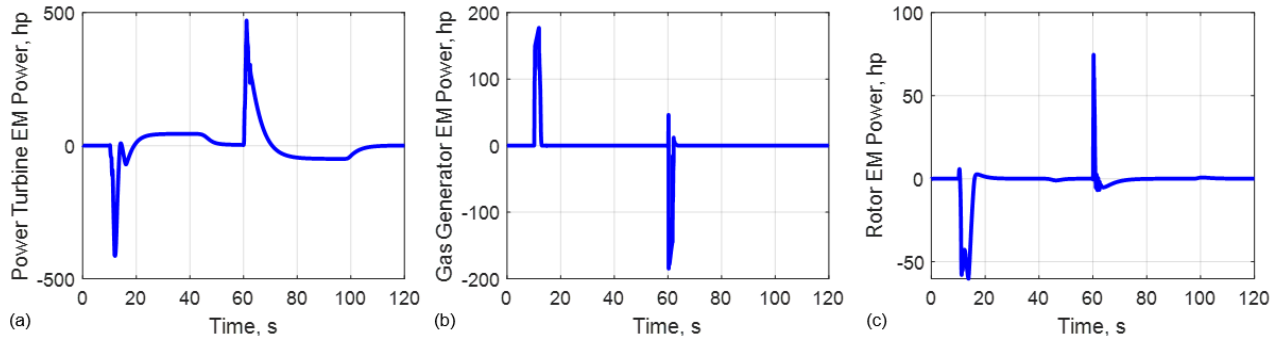


Figure 14. Off-nominal electric machine power inputs with TEEM.

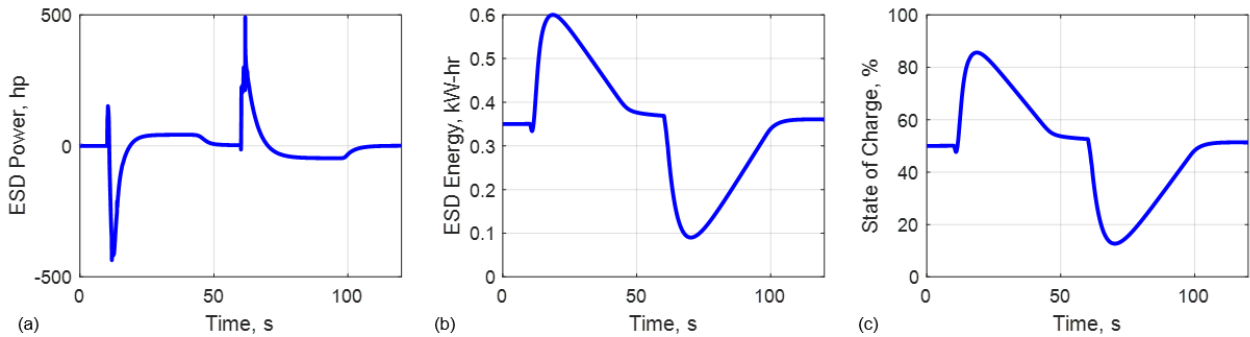


Figure 15. ESD power, energy, and SOC to accommodate operation with TEEM.

An alternative to net power injection during decelerations is to fully or partially deactivate the transient TEEM control logic during decelerations. Given this is a single-spool gas generator, the compressor does not typically move toward stall during deceleration, and so the only purpose the TEEM control logic serves in this instance is to more tightly regulate the power turbine and rotor speeds. If the baseline speed regulation during decelerations is satisfactory, then the TEEM transient control logic could be deactivated to eliminate the need for power injection, which also eliminates the need to re-charge the ESD thus eliminating the increase in fuel burn following deceleration transients. Another potential benefit to this alternative approach is that the nominal SOC could be reduced allowing a reduction in the re-usable ESD energy capacity since there is no need to store energy that is not used.

Thrust augmentation is demonstrated in Fig. 16. Here the PL is increased from 0 to 107 over the course of 1 s. The simulated case is at SLS conditions during hover, where a benefit of increased thrust is shown. The maximum thrust is increased by ~7% while the response time remains similar and superior operability is maintained. This feature may become useful for handling infrequent or temporary situations, thus improving safety and/or enabling the aircraft to meet the demands of a wider range of missions. One example to which this feature could be applied is the transition of the Tilt-Wing from hover to forward flight. Ideally, the vehicle should be able to make the transition at its heaviest load without losing altitude. The integrated flight dynamic and rotor model mentioned prior was utilized to determine the trim conditions as the tilt-wing transitions from hover to forward flight. The aircraft pitch was fixed while the thrust, velocity, and longitudinal cyclic pitch and/or horizontal tail angle were adjusted to maintain steady-level flight. Figure 17 shows the rotor shaft power required to maintain

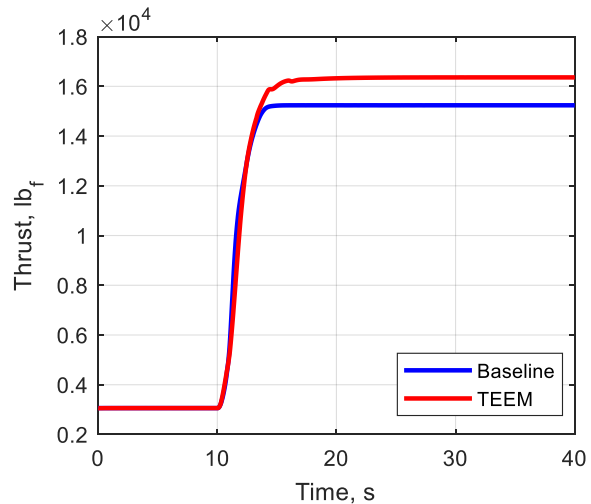


Figure 16. Thrust response with thrust augmentation from energy storage.

steady-level flight for the aircraft during the transition of the Tilt-Wing at an altitude of 5,000 ft and for its designed take-off weight of 13,877 lb_f. The maximum rotor shaft power supplied by the engine is exceeded by roughly 14 hp as the wing transitions between ~50° and ~62.5°. While the power deficit is small, it is not ideal. Rather than resizing the engine or reducing load capacity to accommodate such a temporary situation, electric power augmentation is a potential solution to assuring the desired altitude is maintained during transition.

VIII. Conclusion

Power management in a Tilt-Wing propulsion system was demonstrated to provide several benefits. Simulations demonstrate an appreciable improvement in compressor operability. The primary expected benefit of this is the expansion of the engine design space that could lead to a lighter and/or more efficient engine. Another benefit associated with the energy management techniques employed during transients was the tighter regulation of the power turbine and rotor speeds. The tendency of power turbine and rotor speed regulation controllers to extract power during accelerations and input power during decelerations (if desired) offsets the power needed for maintaining engine operability. This could result in a smaller energy storage system. Excess energy obtained during transients was leveraged to achieve a temporary reduction in fuel burn that can add up over the course of numerous missions for a fleet of these vehicles. In addition, the presence of re-usable energy storage allowed additional power to be applied to the rotors to temporarily increase the maximum thrust by ~7%. Overall, transient operability benefits through TEEM was applicable to this smaller class of commercial air transport. In addition it was shown to provide benefits to hybrid electric propulsion architectures with turbomachinery that primarily produces power. In fact, for this propulsion system architecture, TEEM was shown to provide new benefits that were not applicable to the previously evaluated turbofan engines. Not only was TEEM shown to have the ability to positively impact the turbomachinery, but the entire propulsion system. The ability of TEEM and related power and energy management techniques appears to provide increasing benefits as the propulsion system becomes more distributed and more electrified, with turbomachinery at its core.

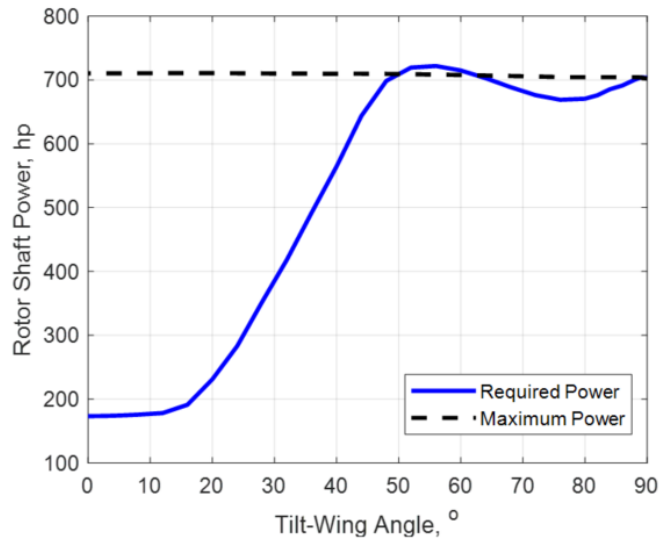


Figure 17. Required rotor shaft power for a level transition between hover and forward flight.

Acknowledgments

The authors would like to thank Jeff Chapman, Mike Tong, and Chris Snyder from the NASA Glenn Research Center. Jeff provided a basis for developing the baseline turboshaft engine model and Mike was kind enough to conduct a weight analysis of the turboshaft engine to provide estimates of the much needed shaft inertias. Chris was helpful in running and interpreting NDARC data used to create and verify the Simulink rotor model. The authors would also like to thank Chris Silva and Wayne Johnson from the NASA Ames Research Center. Chris and Wayne provided insight into the modeling of the Tilt-Wing rotors.

References

- [1] Culley, D., Kratz, J., and Thomas, G., "Turbine Electrified Energy Management (TEEM) For Enabling More Efficient Engine Designs," AIAA Propulsion & Energy Forum, Cincinnati, OH, 2018.
- [2] Kratz, J., Culley, D., Thomas, G., "A Control Strategy for Turbine Electrified Energy Management," AIAA Propulsion & Energy Forum, Indianapolis, IN, 2019.
- [3] Kratz, J., Culley, D., and Thomas, G., "Evaluation of Electrical System Requirements for Implementing Turbine Electrified Energy Management," AIAA Propulsion & Energy Forum, Indianapolis, IN, 2019.
- [4] Bradley, M. K., Droney, C. K., "Subsonic Ultra Green Aircraft Research: Phase II – Volume II – Hybrid Electric Design Exploration," NASA CR-218704, 2015.

-
- [5] Johnson, W., Silva, C., and Solis, E., “Concept Vehicles for VTOL Air Taxi Operations,” American Helicopter Society Conference of Aeromechanics Design for Transformative Vertical Flight, Alexandria, VA. 2018.
- [6] “Guidelines for Analysis of Hybrid Electric Aircraft System Studies”, URL: https://www.aiaa.org/docs/default-source/uploadedfiles/publications/standards/hybrid-electric_properties_attributes.pdf?sfvrsn=c8eb8f11_0
- [7] Chapman, J., Lavelle, T., May, R., Litt, J., and Guo, T.-H., “Toolbox for the Modeling and Analysis of Thermodynamic Systems (T-MATS) User’s Guide,” NASA TM-2014-216638, 2014.
- [8] Tong, M., and Naylor, B., “An Object-Oriented Computer Code for Aircraft Engine Weight Estimation,” ASME Turbo Expo 2008, Berlin, Germany. 2008.
- [9] Johnson, W., “NASA Design and Analysis of Rotorcraft - Theory,” NASA TP-2009-215402. 2009.
- [10] Johnson, W., “NASA Design and Analysis of Rotorcraft – Input,” NASA TP-2015-218751. 2015.
- [11] Johnson, W., “Rotorcraft Aerodynamics Models for a Comprehensive Analysis,” American Helicopter Society Forum, Washington, D.C. 1998.
- [12] FAA Federal Aviation Administration, “Title 14 of the Code of Federal Regulations”, https://www.ecfr.gov/cgi-bin/text-idx?SID=2df09c833c6cae09d18ba3a5ae91abb0&mc=true&node=se14.1.33_173&rgn=div8, accessed January, 2020.